Journal for Technology of Plasticity, Vol. 29 (2004), Number 1-2

ANALYSIS, FEM SIMULATION AND EXPERIMENTAL VERIFICATION OF GEAR COLD EXTRUSION

Miroslav Plančak[1], Marko Skunca[2], Miljenko Math[2]

[1] University of Novi Sad, Serbia and Montenegro
[2] University of Zagreb, Croatia

ABSTRACT

The purpose of this paper is to present the theoretical and experimental investigation of radial cold extrusion of gear-like elements. In the theoretical analysis Upper Bound solution for load and average pressure prediction has been developed.
Furthermore, simulation of radial extrusion of geared part has been performed by FEM, using MSC.Marc 2001 simulation program package. Due to axial symmetry of the problem, numerical simulation was carried out over one twelfth of the cylindrical billet. Tetrahedral body mesh using higher order elements enabled the simulation to run to completion without remeshing. Values of reaction forces summarized over appropriate nodes gave final force - stroke diagram including the final steep load rise coming from simulated corner filling phenomenon.
Finally, experiments were carried out with the aim to verify theoretical prediction and FEM simulation.
Obtained results are compared and analysed. As it has been shown, experimental verification gives well agreeable results to the analysis and FEM simulation, except for the final extrusion phase (corner filling) when Upper Bound prediction underestimates the real load values.
***Keywords**: Gear extrusion, Upper Bound, FE simulation, experiment*

1. INTRODUCTION

Due to its advantage when compared with other manufacturing methods cold extrusion is increasingly gaining in importance, especially for production of small and medium size parts of complex geometries.
In last decades investigations of cold extrusion have been under intensive growth, focusing at various problems, such as:
- application of new materials of the component
- new tool materials
- CAD/CAM techniques
- “net shape forming”

- process modelling and simulation
- increasing the range of component geometries etc.

Since the basic types of cold forging (forward, backward and combined extrusion) have been thoroughly investigated by many researchers, in the field of components with more complex shape there is still often a scarcity of technological information.

Cold extrusion of gear-and gear like elements is one of the typical examples of the “complex shape” extrusion. There are different modes of gear extrusion, one of the most frequently applied being radial or sideways extrusion. This is one operation in which the material is constrained to flow sideways trough an orifice in the container wall, filling up the tool cavity and creating component with secondary shape elements.

Gears– and gear like components manufactured by cold extrusion are characterized by improved cost effectiveness and higher mechanical properties compared with gears made by conventional cutting methods. This is the main reason for the industrial application of this technology.

Number of works have dealt with the problem of gear cold extrusion.

In [1] author investigated possibilities for production of high quality gear teeth. For that purpose special die design has been proposed. It has been shown that by using the proposed technology steps “forming-hardening-hard finishing” high gear quality can be achieved.

Investigation of spline extrusion is presented in [2]. Author concluded that the most influential factors on the filling up of the die cavity are friction, teeth profile and billet diameter. As the result, author derived the optimal parameters of the die cavity and billet geometry.

New precision forging of gears, using the principles of “divided flow” has been proposed by Kondo [3]. Flow relief hole and flow relief axis have been introduced with the effect of load reduction. The concept was applied in the investigation of internal and external gear manufacturing.

Two different modes of radial extrusion have been analysed by Upper Bound in [4]. Impact of billet geometry, friction and workpiece geometry on total load has been discussed.

Extrusion of gear-like components with three different teeth geometries is presented in [5]. The comparison between theoretically and experimentally obtained load-stroke diagram show reasonable agreement up to the final stage of extrusion. In this stage significant discrepancy between theory and experiment exists.

Paper [6] deals with the development of precision forging technology for gear production.

Authors developed the concept of flexible tool system for production of gear parts. Furthermore, stress and forces prediction has been made by using FEM package.

Steps taken in defining and improving the model of radial gear extrusion in cold state using FEM are elaborated in [7]. For that purpose MSC.Marc 2001 simulation program package has been applied to model the process, taking into account following two factors; accordance with experimentally obtained data and numerical properties of the simulation itself. It has been shown that that using higher order element diminishes the problem of overall volume loss - a problem that violates the incompressibility law in FEM simulations of large deformations.

In [8] authors obtained and analysed hardness distribution of gear manufactured by radial cold extrusion. It has been shown that the highest stress and strain values appear around the corner in the transition zone between the tooth base and tooth flank. Stress and strain distribution was obtained by the hardness-strain-stress relationship.

Present paper is concentrated on cold radial extrusion of gear – like components. Attention has been focused on the theoretical investigation, FE simulation and experimental verification of cold radial extrusion of gear – like elements.

2. UPPER BOUND ANALYSIS

The simplified scheme of the sideways (radial) extrusion, together with the extruded geared component, is given in Fig.1. As it can be seen, from the solid cylindrical billet component with 6 straight radial flank profile is obtained by sideways extrusion.
In order to perform Upper Bound analysis the workpiece has been divided into four separate zones (Fig.2a). For each zone velocity field, which obeys incompressibility law and satisfies the boundary conditions has been established. Analytical form of this field is given in the Table 1 and its graphical interpretation in fig 2b.

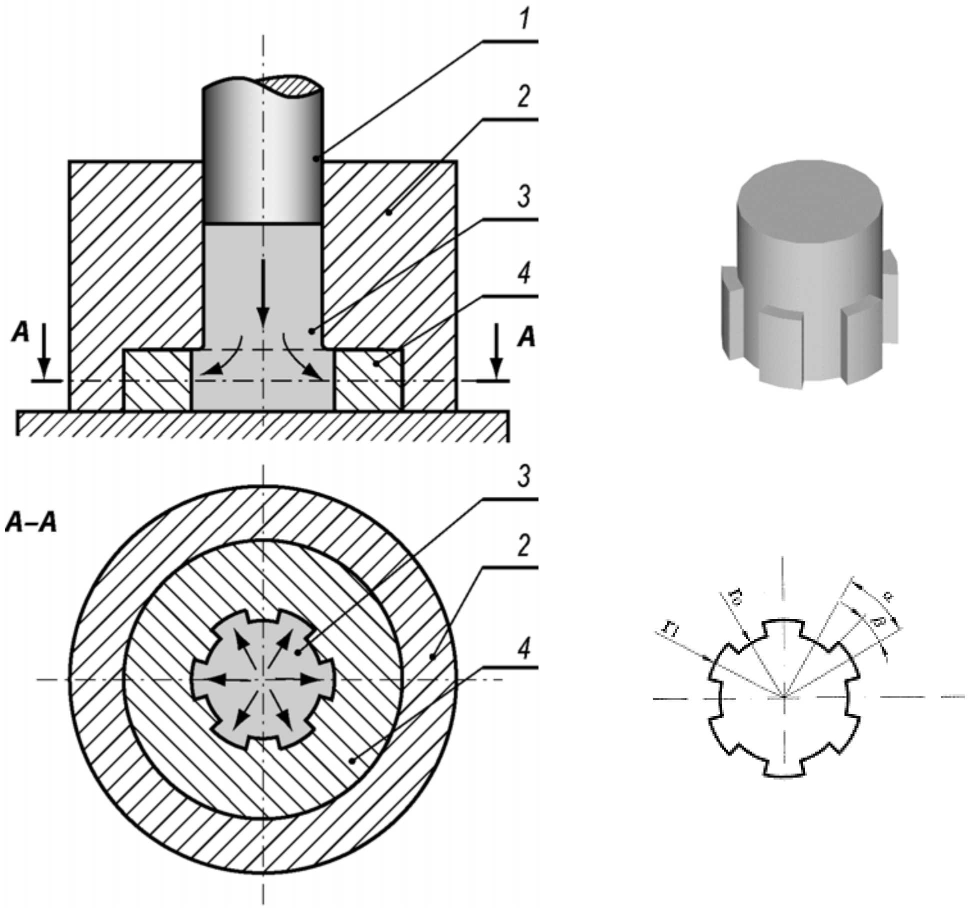

Fig.1. Sideways extrusion and extruded component

1 – punch, 2 – die, 3 – geared component, 4 – die insert

Table 1

	v_z	v_θ	v_r
Zone 1	$-v_0$	0	0
Zone 2	$-v_0 \frac{z}{h}$	$-v_0(\alpha-\theta)\frac{r}{h}$	0
Zone 3	$-v_0 \frac{z}{h}$	$-v_0(\alpha-\beta)\frac{\theta r}{\beta h}$	$v_0 \frac{\alpha r}{2\beta h}$
Zone 4	0	0	$v_0 \frac{r_0^2 \alpha}{2hr\beta}$

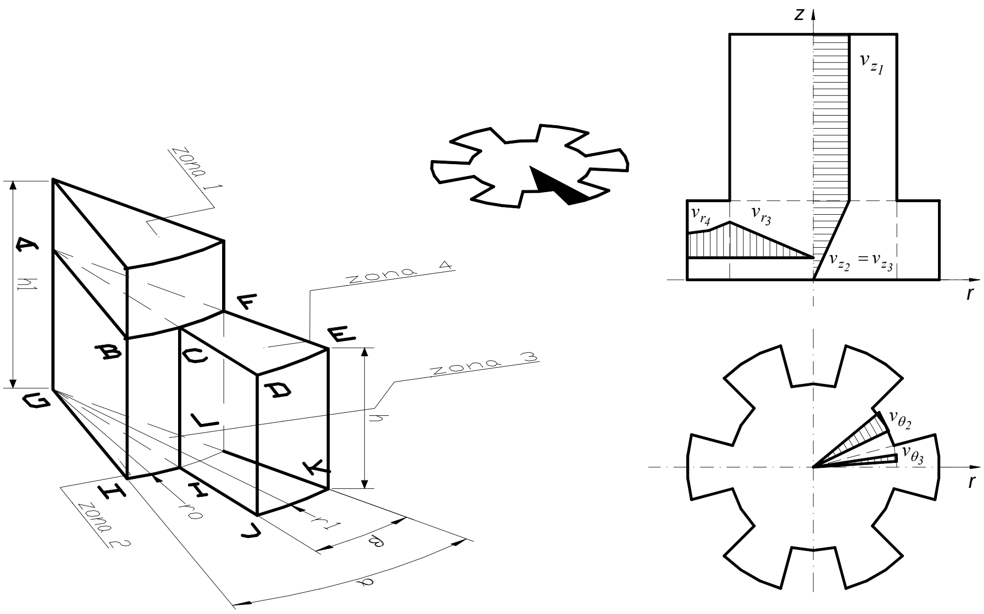

Fig. 2. Different zones of the component and velocity field

Based upon the assumed velocity field, Upper Bound procedure has been carried out. Strain rates for every zone were defined as:

Zone 1 (Rigid zone)

$$\dot{\varepsilon}_{rr} = \dot{\varepsilon}_{\theta\theta} = \dot{\varepsilon}_{zz} = \dot{\varepsilon}_{r\theta} = \dot{\varepsilon}_{\theta z} = \dot{\varepsilon}_{zr} = 0 \quad (1)$$

Zone 2

$$\dot{\varepsilon}_{rr} = 0 \quad \dot{\varepsilon}_{\theta\theta} = \frac{v_0}{h} \quad \dot{\varepsilon}_{zz} = -\frac{v_0}{h} \tag{2}$$

$$\dot{\varepsilon}_{r\theta} = \dot{\varepsilon}_{\theta z} = \dot{\varepsilon}_{zr} = 0$$

Zone 3

$$\dot{\varepsilon}_{rr} = \frac{v_0\alpha}{2h\beta} \quad \dot{\varepsilon}_{\theta\theta} = -\frac{v_0\left(\alpha - 2\beta\right)}{2h\beta} \quad \dot{\varepsilon}_{zz} = -\frac{v_0}{h} \tag{3}$$

$$\dot{\varepsilon}_{r\theta} = \dot{\varepsilon}_{\theta z} = \dot{\varepsilon}_{zr} = 0$$

Zone 4

$$\dot{\varepsilon}_{rr} = -\frac{v_0 r_0^2 \alpha}{2hr^2\beta} \quad \dot{\varepsilon}_{\theta\theta} = \frac{v_0 r_0^2 \alpha}{2hr^2\beta} \quad \dot{\varepsilon}_{zz} = 0 \tag{4}$$

$$\dot{\varepsilon}_{r\theta} = \dot{\varepsilon}_{\theta z} = \dot{\varepsilon}_{zr} = 0$$

Using velocity filed and strain rates field total power was calculated as:

$$\dot{W} = \dot{W}_d + \dot{W}_s + \dot{W}_f = \frac{2\sigma_e}{\sqrt{3}} \int_V \sqrt{\left(\frac{1}{2}\dot{\varepsilon}_{ij}\dot{\varepsilon}_{ij}\right)} dV + \int_{A_s} \tau_s \left|\Delta v\right| dA_s + \int_{A_f} \tau_f \left|\Delta v\right| dA_f \tag{5}$$

σ_e - the yield stress

As it can be seen from (5), the total power consists of three components: internal power of deformation ($\dot{W}_d$), shear losses on the boundaries of velocity discontinuities ($\dot{W}_s$) and friction losses ($\dot{W}_f$), whereas each of the components comprises a certain number of subcomponents. Total power in terms of all subcomponents is given as:

$$\dot{W} = \left(\dot{W}_{d2} + \dot{W}_{d3} + \dot{W}_{d4} + \dot{W}_{s1} + \dot{W}_{s2} + \dot{W}_{s3} + \dot{W}_{s4} + \dot{W}_{f2} + \dot{W}_{f3} + 2\dot{W}_{f4} + \dot{W}_{f5} + \dot{W}_{f6}\right) \cdot$$
$$\cdot 2 \cdot t + \dot{W}_{f1}$$

where are:

- $\dot{W}$ - total power
- $\dot{W}_{d2}$ - power for internal deformation in the zone 2
- $\dot{W}_{d3}$ - power for internal deformation in the zone 3
- $\dot{W}_{d4}$ - power for internal deformation in the zone 4
- $\dot{W}_{s1}$ - shear loss on ABCA surface
- $\dot{W}_{s2}$ - shear loss on ACFA surface
- $\dot{W}_{s3}$ - shear loss on ACIGA surface
- $\dot{W}_{s4}$ - shear loss on CFLIC surface

- $\dot{W}_{f1}$ - friction loss on the outer cylindrical surface of the zone 1
- $\dot{W}_{f2}$ - friction loss on GHIG surface
- $\dot{W}_{f3}$ - friction loss on GILG surface
- $\dot{W}_{f4}$ - friction loss on CDEFC (or IJKLI) surface
- $\dot{W}_{f5}$ - friction loss BCIHB surface
- $\dot{W}_{f6}$ - friction loss on CDJIC surface
- t – number of teeth

(For the notation please refer to the figure 2.)

The complete derivation of each subcomponent can be found elsewhere [4], [7].

Total force is:

$$F = \frac{\dot{W}}{v_0}$$

and average punch pressure:

$$p = \frac{F}{A}$$

Prediction of load-stroke diagram (Fig. 3) obtained by the developed Upper Bound solution has been applied for the following gear geometry:

- inner radius r_0: 14mm
- outer radius r_1: 17mm
- tooth height h: 15.8mm
- angles $\alpha = \pi/6$, $\beta=\pi/12$, $\psi=\pi/6$
- friction coefficient $\mu = 0.12$
- Yield stress: = 82.3 MPa
- number of teeth t: 6

3. FE SIMULATION

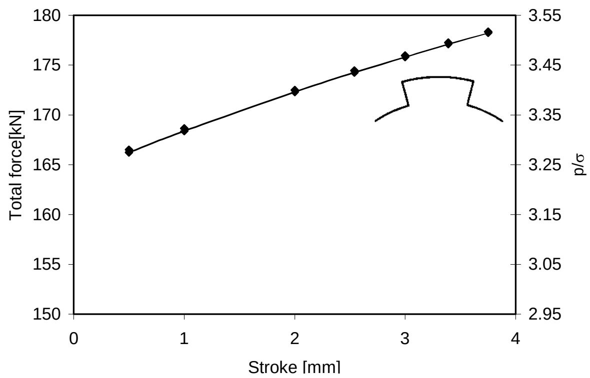

Fig.3. Load-stroke and average pressure-stroke diagram: Upper Bound prediction

Simulation of radial gear extrusion was done on one twelfth of the gear using the same dimensions as in upper bound method. Created in pre-processor, initial geometry is relatively simple and includes four contact bodies as shown on Fig. 4a. To keep the problem as simple as possible, only the billet was subdivided into the tetrahedral mesh. Refinement of the mesh towards the outer billet radius was created primarily to enhance the element resolution around cavity corners, making material flow around them appropriate. Preceding simulations have exhibited a big force - stroke oscillations coming from sudden entrance of nodes into the gear cavity. Nodes entering the gear cavity induce sudden change of their contact status from 1 to 0. This change immediately alters the values of the load vector **r** making the non-linear system presented by a stiffness equation (6) to be necessarily resolved by additional number of Newton Raphson iteration cycles in the current increment. All existing force - stroke diagram jumps come from mentioned change of contact when nodes come in or out (splitting) of contact.

$$K\ v = r \qquad (6)$$

K - Global stiffness matrix
v - Global displacement vector
r - Global Load vector

In order to produce an applicable solutions i.e. to record force - stroke diagram, constitutive equations including yield criteria have to be applied onto the particular geometry. Therefore a set of boundary conditions was set up on all the nodes lying in two axisyimmetric planes. Together with rigid contact bodies: Punch, Lower plate and Container, those boundary conditions restrained the simulated material flow, to the one twelfth of the gear geometry. Less sensitive to the large deformations than linear elements, selected parabolic elements (Fig. 5b) sustained severe mesh distortion even performing a corner filling phenomenon at the very end of the simulation. Deformed shape as a result shows a satisfactory container cavity fulfilment without any mesh refinement technique used (Fig. 4b).

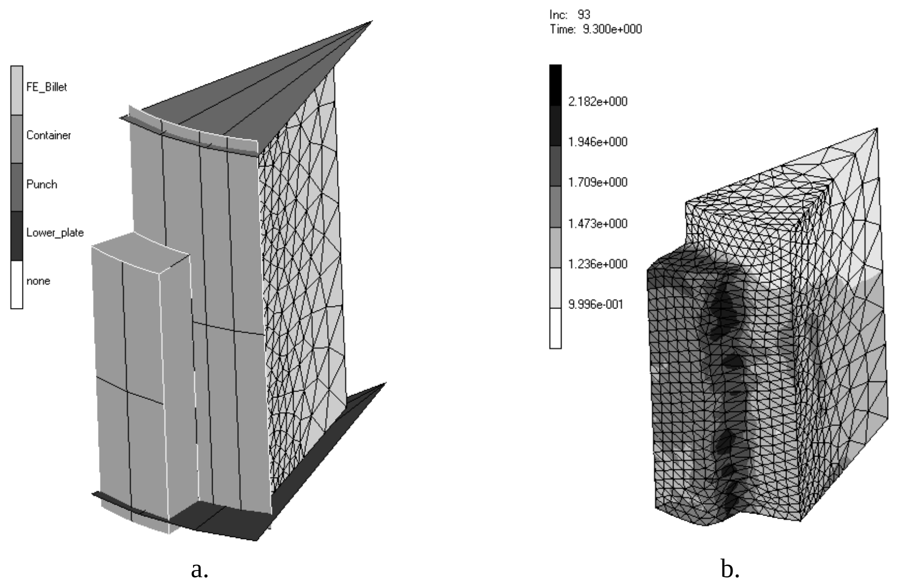

a. b.

Fig 4. Four contact bodies included in FE simulation (a). Good container cavity fulfilment after 93 increments (b). Contour bands showing Equivalent Stress/Yield Stress.

The material assigned to element mesh was modelled as time independent rigid plastic material, with the initial yield stress 82 N/mm^2. Although the assumption of rigid plastic flow was made, model experienced overall element volume loss of 1% that came from FE mesh distortion (Fig. 5c). Flowchart was assigned to the 99.5% Al material model accordingly to [11].
Since the process of radial extrusion belongs to the non-stationary large deformation problem, its kinematics was described using Lagrangian approach. The nodes attached to the initial billet segment move through the space along with the material. Although the identification of coordinates is made for undeformed geometry at the very beginning of simulation, integration of equilibrium equations over the increments has to be done for the current configuration. Since plastic deformations and displacements are large, current state has a little in common with initial state. Therefore equilibrium equations have to be rewritten in current frame of reference. This method is known as Updated Lagrange procedure as discussed in [10] and it was used in solving presented example.

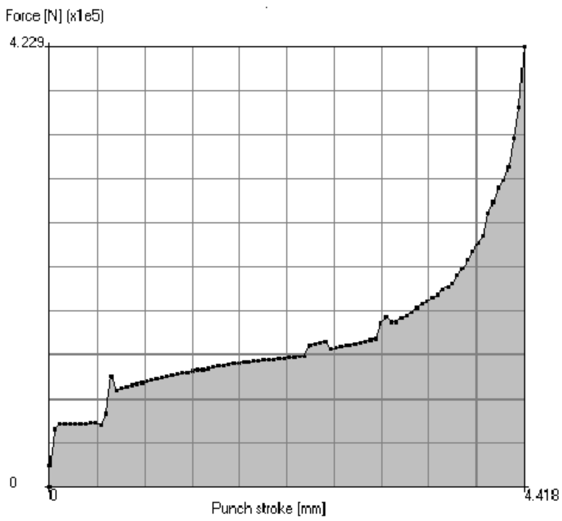

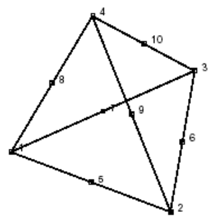

b.

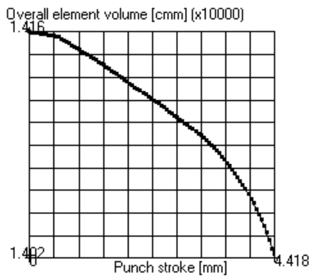

a. c.

Fig 5. Numerically obtained force - stroke diagram (a). Tetrahedral, parabolic element type used in simulation (b). Overall element volume decreases with mesh distortion up to the final volume loss of 1% (c)

Lack of reference state implies the use of numerical criteria that has to be satisfied before simulation can proceed to the next increment. In our case relative residual force check has been used as condition of recycling the increment or proceeding to the next one. Residual force checking resulted in 545 Newton Raphson iteration cycles performed in simulation. Additional numerical check on conditioning of the equilibrium equations was provided by Marc that is calculating the singularity ratio of stiffness matrix right after its assembly. In actual simulation all calculated singularity ratio values remained in satisfactory interval between 10^{-4} and 1, therefore after [9] we can assume that the conditioning of the equilibrium equations is good.
As mentioned before, all the force - stroke jumps on Fig. 5a come from change of contact status. First jump at the very beginning of simulation happens when Punch comes in sudden contact with FE Billet changing the contact status of all top end nodes from 0 to 1. Second jump comes from

similar situation when outer radius FE Billet comes in contact with the Container surface Fig. 4a. Force jump at stroke amount 2.38 mm comes from group of 6 nodes coming out of contact (separation) at the top of the gear cavity at h = 15.8 mm, bringing additional nonlinearity to the stiffness equation (6). Force jump at 3.04 mm comes from realization of contact inside gear cavity. Together with numerical criteria satisfied and the force jumps correlated to contact status, the force - stroke diagram shown on Fig. 5a can be considered good and reliable to be compared with experimental data.

4. EXPERIMENTAL VERIFICATION

Experimental investigations were conducted on the hydraulic Sack and Kiesselbach 6300kN press, by using the special tooling, shown in Fig.6.
The main tooling elements are the punch, the die and the die insert, provided by geared profiles. The billet with the geometry: ∅28 x 40 mm was prepared out of Al99.5 which strain-stress curve was obtained in Rastegaev test. Analytical form of this curve is:

$$\sigma = 152.49 \cdot \varepsilon^{0.292} \left[\text{MPa}\right]$$

Billet was placed into the die and forced by punch to fill up the geared cavities in the die insert. Process was performed incrementally in 6 steps. After every step load was measured, tooling was partly dismantled and photographs of instantaneous die filling are made.
Experimentally obtained load-stroke dependence, with corresponding photographs of the die filling degree in every increment is given in Fig.7.

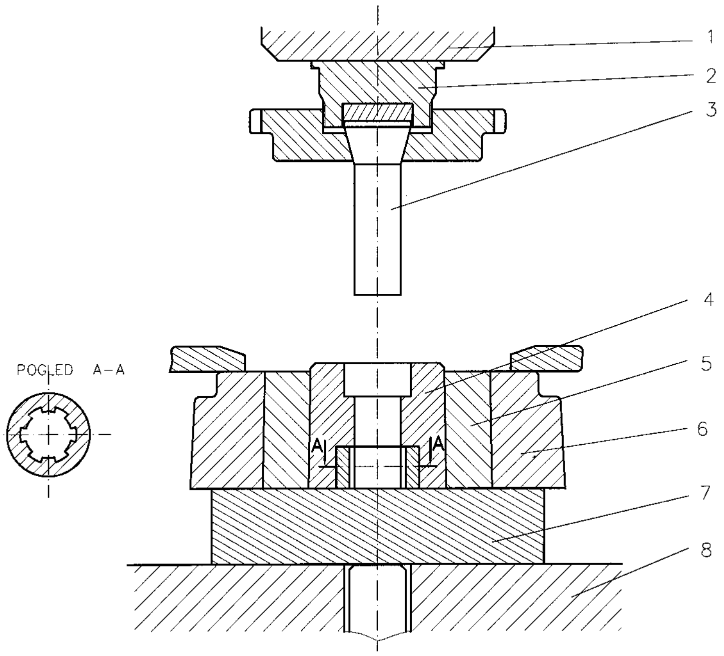

Figure 6. Experimental tooling
1. Upper plate, 2 Punch holder, 3 Punch, 4 Container, 5 Inner ring, 6 outer ring,
7 Lower plate, 8. Press

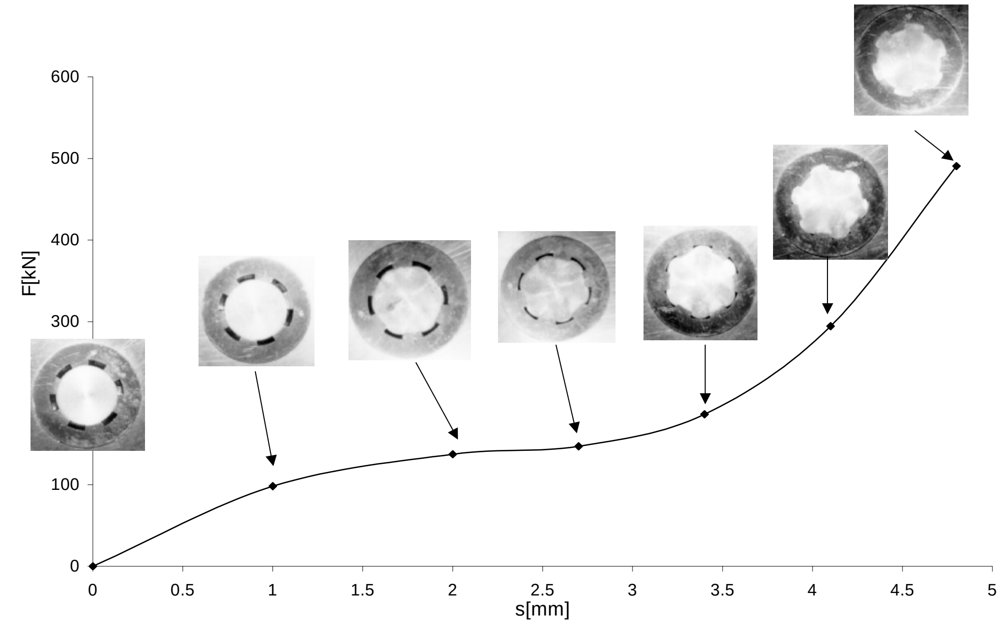

Fig. 7. Experimentally obtained load – stroke diagram with the corresponding die filling degree

5. DISCUSSION

A direct comparison of the load – stroke diagram obtained by:

- Upper Bound (UB) method
- FEM simulation and
- Experimentally

is given in Fig.8.

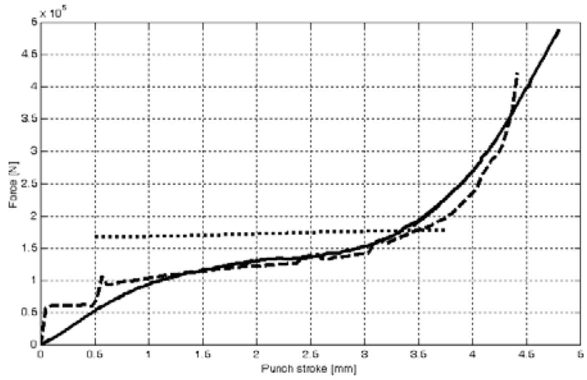

Fig. 8. Load-stroke diagram obtained by three different methods.

Experimentally obtained load (solid line), FE simulation obtained load (dashed line) and Upper bound obtained load (dotted line).

Diagram obtained by Upper Bound is characterized by steady, low rise of extrusion load throughout the entire process, without any inflexions. Up to the punch stroke of 2.5 mm load values predicted by Upper Bound are approximately 20% higher than those obtained by other two methods. This overestimation can be explained by the inherent nature of UB technique. In the final stage experimental and simulated loads are considerably higher than UB prediction.

Load-stroke relationship obtained by FEM simulation shows explainable behaviour, coming from the fact that in FE simulation of radial extrusion; we are dealing with discretized continuum. Since numerical criteria set upon simulation was satisfied, the results obtained in dealing with geometrical nonlinearity, can be considered as satisfactory ones. Large force jumps at the very beginning of simulation were not considered as problematic, since after the realization of a full contact between FE Billet and Container, simulation performs good and physicaly explainable numerical behaviour. At the punch stroke of 3.04 mm starts expected contact inside gear cavity coinciding with second inflexion point in experimentally obtained load Fig. 8. Final steep load rise comes from simulation of corner filling phenomenon obtained to a satisfying extent without remeshing.

Experimentally obtained load-stroke diagram resembles to great extend this obtained by FEM simulation. Initially, load increases quickly up to the punch stroke of approximately 1 mm. As the punch stroke proceeds, the load continues to increase at lesser rate. Final phase is characterized by steep load rise.

Certain discrepancy between the predicted load (UB) and load obtained by simulation and by experiment can be attributed to the simplified velocity field assumed for the Upper Bound analysis. This field does not take into account the phenomenon of corner filling which occurs in the final extrusion phase and which is responsible for the steep load jump.

Further work on this subject should be bound with the improvement of the velocity field for Upper Bound prediction. Also, it is planed to extend the investigation on other, more complex component geometries, preferably parts for automotive industry, such as spiders, helical teeth component, cross groove inner race etc. Future FE simulations of mentioned geometries shall include the friction models using gap and friction elements and tetrahedral remeshing methods available in latest version of MSC.Marc2003. The use other program packages able to cope with problems of radial extrusion will be also considered.

Acknowledgements

This work was supported by Ministry for science, technology and development of Republic of Serbia.

6. REFERENCES

[1] Dohmann, F., Meier, T., Production Sequence Forming – Hardening – Hard Finishing for the Manufacture of Ready – to – install – Gearing, Proceedings of 9th International Cold Forging Congress, Solihull, U.K., p. 169-177, 1995.

[2] Lili, J., An upper bound analysis for extrusion of splines, Advanced Technology of plasticity, p. 582-586, 1993.

[3] Kondo, K., Development of New Precision Cold Die Forging Processes, 1st ICTP, Tokyo, p. 876-887, 1984.

[4] Plancak M., Vujovic V., Vilotic D.: Ein Beitrag zur Untersuchung von Querfliesspressen – XXIV Kolloquium Kaltmassivumformung, Zwickau, 1987.

[5] Skakun, P., A contribution to the investigation of cold extrusion of complex shapes, M. S. thesis, Novi Sad, Yugoslavia 2001.

[6] Rodrigues J.M.C., Gracio J.J., Martins P.A.F.: Precision forging of gears: experimental and theoretical investigation, IV Conferencia International de Forjamento / Brazil, Editor L. Scheaffer, 2001.

[7] Plancak M., Skunca M., Math M.: Numerical simulation of radial gear extrusion in cold state, 9th International Scientific Conference on Production Engineering, CIM - Computer Integrated Manufacturing, June 05 / 06 2003. Lumbarda, Croatia.

[8] Plancak M., Vilotic D., Vujovic V.: One contribution to the investigation of gear extrusion, 5th International Conference on Technology of Plasticity, Columbus, Ohio, USA, 1996.

[9] MARC – Primer (Rev K.5), MARC Analysis Research Corporation, Palo Alto, California, Printed in USA, 1993.

[10] MARC – Volume A (Version K7), MARC Analysis Research Corporation, Palo Alto, California, Printed in USA, 1997.

[11] ADB - AWF «Fliesskurven metallischer Werkstoffe» VDI 5-3200, Oktober 1954

ANALITIČKO ISTRAŽIVANJE, FE SIMULACIJA I EKSPERIMENTALNA VERIFIKACIJA PROCESA HLADNOG ISTISKIVANJA ZUPČANIKA

Miroslav Plančak, Marko Skunca, Miljenko Math

REZIME

U radu su prikazana teoretska istraživanja procesa hladnog istiskivanja elemenata sa ozubljenjem. Korišćena je metoda gornje granice. Radni komad je bio podeljen u četiri odvojene zone za koje su definisane kinematski dozvoljena polja brzina, respektujući granične uslove. Korišćenjem standardne procedure gornje granice dobijeni su svi elementi ukupno potrebne snage i sile za deformisanje.
Proces je analiziran i metodom konačnih elemenata (FE). U tu svrhu analizirana je dvanaestina dela (zbog simetrije), korišćenjem programa MSC. MARC 2001 paketa. Proces je izveden bez remeshing-a obzirom da je u simulaciji korišćena tetraedarna mreža višeg reda. Materijal je bio smatran za kruto-plastičan sa inicijalnim naponom tečenja $\sigma_y = 82$ N/mm^2.

Za potrebe eksperimentalne verifikacije rezultatata dobijenih gornjo-graničnom analizom i FE-simulacijom, izvršena su i eksperimentalna istraživanja. U tu svrhu konstruisan je i izrađen specijalan alat koji je imao umetak – negativ istisnutog elementa. Analizirani materijal je bio Al99,5 sa krivom tečenja

$$\sigma = 152.49\,\varepsilon^{0.292} \text{ [MPa]}$$

Upoređenje rezultata (sila – put dijagram) ukazuje na sledeće:

- *gornja granica daje rezultate za silu koji su ≈20% veći od FE i eksperimenta*
- *tek u završnoj fazi FE i eksperiment daju nagli skok sile koji se može objasniti fenomenom ispunjenja uglova (“corner fillings”)*
- *određena diskrepancija između gornjo-graničnog rešenja i FE i eksperimenta se može objasniti činjenicom da polje brzina, koje je korišćeno u analizi ne opisuje na zadovoljavajući način posledenju fazu procesa tj. ispunjenje uglova profila zuba. U tom smislu planira se poboljšanje polja brzina koje bi dalo realističnije rezultate.*